Interferometric, Target-Enclosing Waveform Inversion: a Comparison of Approaches

Interferometric, target-enclosing waveform inversion: a comparison of approaches

Introduction

Target-oriented full-waveform inversion methods are becoming increasingly popular under the promise of obtaining high-resolution local subsurface property models at a significantly reduced cost. This is particularly attractive in applications such as reservoir characterization and time-lapse inversion, where the macro velocity model is already known. A number of approaches have been proposed relying on local solvers (e.g. Willemsen et al., 2016), and model-driven, data-driven or hybrid redatuming (da Costa et al., 2019; Cui et al., 2020; Guo and Alkhalifah, 2020). Except for the method of Cui et al. (2020), these methods are not truly local, as in theory they require estimation of the model parameters in an infinite half space below the datum of interest.

Recently, Vasconcelos et al. (2017) proposed a new interferometric objective function, in which the misfit between the pressure wavefields extrapolated in the local subdomain of interest is evaluated, where etrapolation is performed using both the convolution and correlation representation formulas. This new approach is based on the equivalence of the convolution and correlation extrapolated wavefields, up to the time direction, if the subsurface model parameters in the local subdomain are exactly known, whilst errors can be used to guide the inversion process. The convolution and correlation extrapolation formulas require knowledge of the acoustic wavefield on the boundary completely enclosing the area of interest. However, since wavefield extrapolation reproduces the fields only inside the local subdomain, the knowledge of the model parameters outside of the subdomain is not necessary, and in this sense this approach is truly local. Based on the new objective function of Vasconcelos et al. (2017), we formulate an interferometric full waveform inversion (IFWI) method, where the forward and adjoint modelling equations are expressed as integral constraints. We implement the inversion algorithm using the L-BFGS optimization engine and compare its performance with that of the local FWI method of Cui et al. (2020) and the conventional full-domain surface-data FWI both in terms of resolution and computational cost.

Method

The following objective function is minimized in the local subdomain D over squared slowness $m(\mathbf{x})$:

$$I = \frac{1}{2}\sum_s \int_0^T dt \int_D dV \, \|p^{corr}(\mathbf{x},t) - p^{conv}(\mathbf{x},t)\|_2^2 \tag{1}$$

where p^{conv}, p^{corr} are the convolution and correlation pressure wavefields at $\mathbf{x} \in D$, where D is the local subdomain of interest. The convolution and correlation wavefields are constructed by forward and inverse extrapolation of the source wavefield from the boundary ∂D of the subdomain D according to representation formulas:

$$p^{conv}(\mathbf{x},t) = -\int_{\partial D} \left(G^{p,q}(\mathbf{x},\mathbf{x}_r,t) * \mathbf{v}(\mathbf{x}_r,t) + G^{p,f}(\mathbf{x},\mathbf{x}_r,t) * p(\mathbf{x}_r,t)\right) \cdot \mathbf{n}(\mathbf{x}_r)\, dS_r \tag{2}$$

$$p^{corr}(\mathbf{x},t) = \int_{\partial D} \left(G^{p,q}(\mathbf{x},\mathbf{x}_r,T-t) * \mathbf{v}(\mathbf{x}_r,t) - G^{p,f}(\mathbf{x},\mathbf{x}_r,T-t) * p(\mathbf{x}_r,t)\right) \cdot \mathbf{n}(\mathbf{x}_r)\, dS_r \tag{3}$$

where $p(\mathbf{x}_r,t), \mathbf{v}(\mathbf{x}_r,t)$ are pressure and particle velocity at $\mathbf{x}_r \in \partial D$ due to a physical surface source at $\mathbf{x}_s \notin D$, and $G^{p,q}$ and $G^{p,f}$ are components of the vector-acoustic Green's matrix, representing pressure at $\mathbf{x}$ due to an impulsive volume injection and body force sources at $\mathbf{x}_r$, and $\mathbf{n}$ is the outward normal to ∂D. We assume that p and $\mathbf{v}$ solve the constant density vector acoustic system:

$$\begin{aligned} m(\mathbf{x})\partial_t p(\mathbf{x},t) + \nabla \cdot \mathbf{v}(\mathbf{x},t) &= \delta(\mathbf{x}-\mathbf{x}_s)\partial_t q(t) \\ \partial_t \mathbf{v}(\mathbf{x},t) + \nabla p(\mathbf{x},t) &= \delta(\mathbf{x}-\mathbf{x}_s)\mathbf{f}(t) \end{aligned} \tag{4}$$

with the zero initial conditions at $t = 0$ s, where the traces are recorded until $t = T$s. The redatumed boundary wavefields constitute the measured data for the IFWI inversion probelm and equations (2), (3) constitute the constraints.

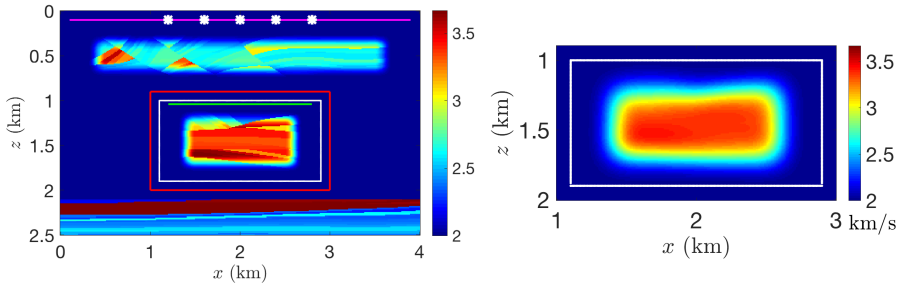

(a) (b)

Figure 1: (a) True velocity model. White stars denotes physical sources; magenta line is physical receivers at every 10 m; red line delineates the domain for the local calculations; white line is the boundary ∂D; green line is the virtual receivers for Cui et al. (2020) method.

The gradient of the objective function (1) is given by

$$\frac{\partial I}{\partial m}(\mathbf{x}) = -\int_0^T [p^{corr}(\mathbf{x},t)p^{corr\dagger}(\mathbf{x},t) + p^{conv}(\mathbf{x},t)p^{conv\dagger}(\mathbf{x},t)]dt \tag{5}$$

for $\mathbf{x} \in D$, where $p^{conv\dagger}, p^{corr\dagger}$ are adjoint convolution and correlation pressure fields that solve the corresponding adjoint problems in integral form:

$$p^{conv\dagger}(\mathbf{x},t) = -\int_D G^{p,q}(\mathbf{x},\mathbf{x}',T-t) * \partial_t(p^{corr}(\mathbf{x}',t) - p^{conv}(\mathbf{x}',t))dV' \tag{6}$$

$$p^{corr\dagger}(\mathbf{x},t) = \int_D G^{p,q}(\mathbf{x},\mathbf{x}',t) * \partial_t(p^{corr}(\mathbf{x}',t) - p^{conv}(\mathbf{x}',t))dV' \tag{7}$$

for each $\mathbf{x},\mathbf{x}' \in D$ and $t \in (0,T)$. In practice, equations (2), (3), (6) and (7) are evaluated by solving the corresponding differential equations, where areal sources are used for equations (2), (3) and volumetric sources for equations (6), (7). In this case, p^{conv} and $p^{corr\dagger}$ are evaluated forward in time, while p^{corr} and $p^{conv\dagger}$ are evaluated backward in time. In the following sections, we give an estimate of the cost of the proposed method and compare its performance to the convolution local FWI method of Cui et al. (2020) and the full-domain surface FWI.

Examples

The true model and geometry used to demonstrate the proposed IFWI method is shown in Figure 1 (a). We use five physical surface sources (white stars in Figure 1) to directly generate the exact boundary data at ∂D (white line). In practice, such boundary measurements can be obtained by redatuming the surface data to the local boundary using, e.g. Marchenko redatuming (van der Neut et al., 2015; Ravasi, 2017). The local and adjoint convolution and correlation extrapolations (equations 2, 3, 6 and 7) are performed in the local subdomain delineated by the red box. The initial velocity model is obtained by Gaussian smoothing of the true model, and the local part of it is shown in Figure 1 (b).

In the local convolution FWI method of Cui et al. (2020), forward modelling is replaced by extrapolation of pressure in D from the redatumed boundary data using the convolution representation formula (2). This is equivalent to conventional FWI applied inside the local subdomain, where the extrapolated convolution wavefield replaces the modelled wavefield. The misfit between the convolution field and the directly redatumed pressure at a set of virtual receivers near the top of the local subdomain (green line in Figure 1 a) is minimized. Thus, the redatumed data at the virtual receivers constitute the measurements, and equation (2) represents the forward modelling constraint. Conceptually, this is different from our method, but is similar in the use of the representation formulas for modelling, which makes both methods truly local.

Figures 2 (a), (b) show gradient updates at the first iteration for our proposed IFWI and local convolution FWI methods. For comparison, Figure 2 (c) shows the local part of the conventional surface-data FWI

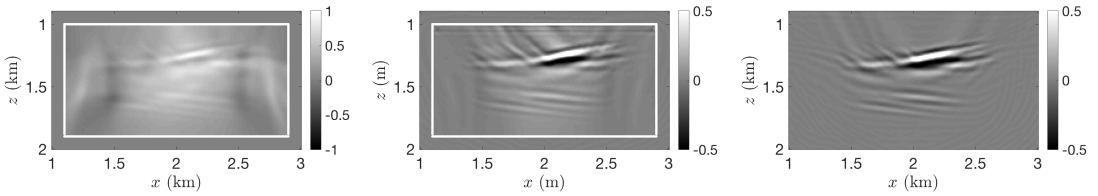

(a) (b) (c)

Figure 2: Gradient updates generated from five sources: (a) IFWI gradient update, (b) local FWI gradient update, (c) conventional surface FWI update.

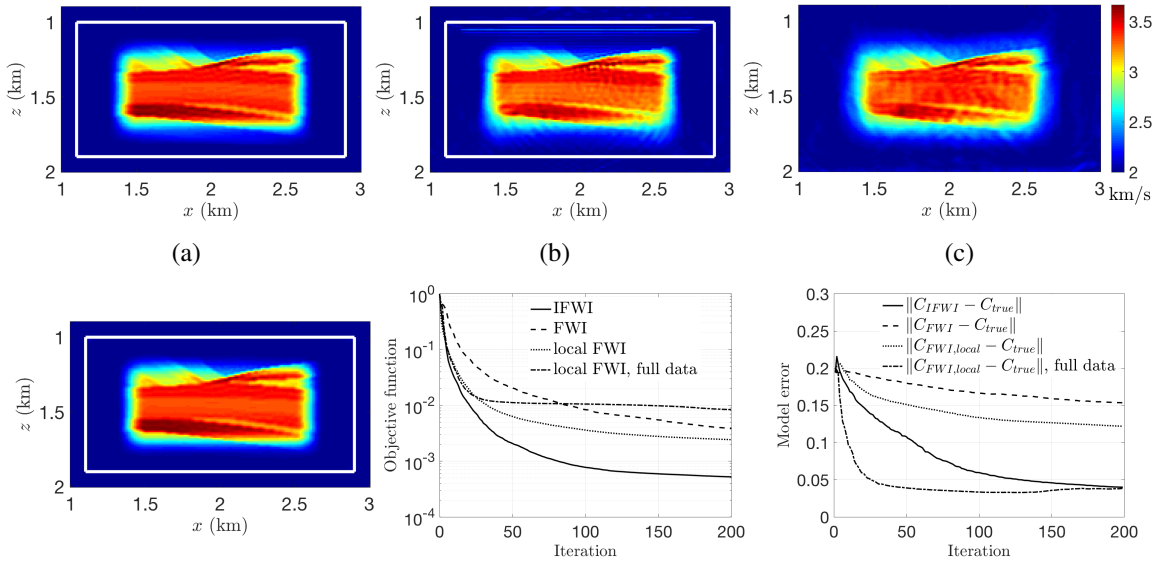

(a) (b) (c)

(d) (e) (f)

Figure 3: Inversion results for: (a) IFWI after 100 iterations; (b) local convolution-based FWI after 200 iterations; (c) surface-data FWI after 200 iterations; (d) local convolution-based FWI with the misfit calculated at every point in the local subdomain after 50 iterations of LBFGS; (e) objective function with iteration and (f) model error with iteration.

gradient update, where the data are modelled using the smoothed whole model in Figure 1 (a) and the misfit is computed at the surface receivers denoted by the magenta line. The IFWI gradient is dominated by low wavenumber components. This is due to the presence of the transmitted waves in the correlation field. Transmitted waves travelling from the bottom reflector to the receivers are also present in the convolution field, and they show up as low wavenumber components in the local convolution FWI update as well, albeit to a lesser extent. This tendency persists at the more advanced iterations of inversion. In the FWI gradient update, transmitted waves are not modelled at early iterations due to the smoothing of the bottom reflector, instead they appear in the gradient at the later iterations, as the reflector below the target area is refined.

Figure 3 shows inversion results obtained by (a) IFWI after 100 iterations, (b) convolution local FWI after 200 iterations, and (c) full-domain surface-data FWI after 200 iterations. Figures 3 (e), (f) show the objective functions and model error norms up to iteration 200. IFWI reconstructs the model with higher resolution than that from both of the other inversions.

Finally, the cost of the different inversion algorithms can be estimated based on the computational complexity of mathematical operations involved. Assuming that N and n is the size in grid points of the global and local domain in each dimension, d is the number of dimensions, and that N_s, N_r and n_t are the numbers of sources, receivers and time-steps, and $n_{red} \propto n^{d-1}$ is the number of points to redatum to, the cost of one IFWI iteration is $O(n^d n_t N_s)$, a half of this for local convolution FWI, and $O(N^d n_t N_s)$ for full-domain FWI. The redatuming cost for both local methods is $O(n_{red} N^{2(d-1)} n_t)$, and is a little

higher for local convolution FWI due to redatuming to the virtual receivers (green line) in addition to redatuming to the subdomain boundary (white line). Based on this, we can conclude that IWFI and local convolution FWI results in Figures 3 (a) and (b) are achieved at the same cost, which is lower than the cost of the full surface FWI, Figure 3 (c).

In principle, local methods are not constrained with respect to the positions where the objective function is evaluated. With this in mind, Figure 2 (d) shows the local convolution FWI result with the misfit evaluated everywhere in the local domain, which makes the problem essentially linear. The objective and model error curves for this inversion are also shown in Figures 3 (e), (f) in dash-dot line. The result has slightly higher resolution than our method's result, and is achieved at 1/4 of the inversion cost of our method. However, in practice such inversion entails redatuming pressure wavefields to every point in the local subdomain, making $n_{red} \propto n^d$, and increasing redatuming cost to $O(n^d N^{2(d-1)} n_t)$, which is likely to be more expensive in 2D and much more expensive in 3D than the additional inversion cost of the proposed IFWI method.

Conclusions

We presented a target-enclosing interferometric full waveform inversion method, where the objective function is the difference between the convolution and correlation wavefields extrapolated from the boundary of a local subsurface subdomain. We evaluated its performance on a synthetic example with exact boundary wavefields. The proposed method is shown to produce higher resolution local velocity models than local convolution-based FWI and full-domain surface-data FWI at a comparable or lower cost. It must be noted that in practice, measurements of the full acoustic wavefield on the enclosing boundary in the local subdomain are not directly available. Such measurements could however be obtained by Marchenko redatuming of surface data. Since this redatuming method requires an accurate kinematic velocity model of the overburden to estimate the initial transmission response, IFWI is mostly suited for local subsurface model refinement. Its robustness with respect to redatuming errors will be subject of future work.

Acknowledgements

The authors thank King Abdullah University of Science and Technology (KAUST) for funding this work. For computer time, this research used the resources of the Supercomputing Laboratory at King Abdullah University of Science & Technology (KAUST) in Thuwal, Saudi Arabia. Alison Malcolm thanks NSERC, Chevron and InnovateNL for funding.

References

da Costa, C.A., Costa, J.C., Medeiros, W.E., Verschuur, D. and Soni, A.K. [2019] Target-level waveform inversion: a prospective application of the convolution-type representation for the acoustic wavefield. *Geophysical Prospecting*, **67**(1), 69–84.

Cui, T., Rickett, J., Vasconcelos, I. and Veitch, B. [2020] Target-oriented full-waveform inversion using Marchenko redatumed wavefields. *Geophysical Journal International*, **223**(2), 792–810.

Guo, Q. and Alkhalifah, T. [2020] Target-oriented waveform redatuming and high-resolution inversion: Role of the overburden. *Geophysics*, **85**(6), R525–R536.

van der Neut, J., Vasconcelos, I. and Wapenaar, K. [2015] On Green's function retrieval by iterative substitution of the coupled Marchenko equations. *Geophysical Journal International*, **203**(2), 792–813.

Ravasi, M. [2017] Rayleigh-Marchenko redatuming for target-oriented, true-amplitude imaging. *Geophysics*, **82**(6), S439–S452.

Vasconcelos, I., Ravasi, M. and van der Neut, J. [2017] Subsurface-domain, interferometric objective functions for target-oriented waveform inversion. *Geophysics*, **82**(4), A37–A41.

Willemsen, B., Malcolm, A. and Lewis, W. [2016] A numerically exact local solver applied to salt boundary inversion in seismic full-waveform inversion. *Geophysical Journal International*, **204**(3), 1703–1720.